We are IntechOpen, the world's leading publisher of Open Access books Built by scientists, for scientists

4,800
Open access books available

122,000
International authors and editors

135M
Downloads

Our authors are among the

154
Countries delivered to

TOP 1%
most cited scientists

12.2%
Contributors from top 500 universities

CLARIVATE ANALYTICS BOOK CITATION INDEX INDEXED

WEB OF SCIENCE™

Selection of our books indexed in the Book Citation Index in Web of Science™ Core Collection (BKCI)

Interested in publishing with us?
Contact book.department@intechopen.com

Numbers displayed above are based on latest data collected.
For more information visit www.intechopen.com

Chapter 4

Adsorption of Heavy Metal onto the Materials Prepared by Biomass

Naoki Kano

Additional information is available at the end of the chapter

http://dx.doi.org/10.5772/61507

1. Introduction

The amount of heavy metal ions released into the environment has been increased due to industrial activities and technological development. Furthermore, indiscriminate disposal has caused worldwide concern for many years because of the toxicity, accumulation in the food chain, persistence in nature, and concentration by organisms [1–3]. Heavy metals are not biodegradable and tend to accumulate in living organisms, causing various diseases and disorders [4, 5]. It is, therefore, important to reduce the levels of toxic metals or to completely remove them from wastewaters before being discharged into the environment [6]. Then, the minimization and assessment of harmful pollutants such as lead (Pb) and uranium (U) in the environment are very significant from the viewpoint of environmental protection.

There are many processes for the treatment of metal-contaminated wastewaters, including chemical precipitation, membrane filtration, reverse osmosis, ion exchange, and adsorption. However, their use is limited due to various disadvantages [7]. Adsorption has been proved as one of the most efficient methods for the removal of heavy metals from aqueous media [8].

Recently, adsorption based on carbonaceous materials including activated carbon (AC) [9], biochar [10], and carbon nanotubes [11] has been gradually applied to this area. Activated carbon has shown great potential for the removal of various inorganic and organic pollutants and radionuclides due to properties such as large surface area, microporous structure, and high adsorption capacity. As a promising material among nanostructured carbon materials, powdered activated charcoal continues to attract tremendous attention due to its unique physical and chemical properties [3, 12]. In particular, the chemical functionalization of activated carbon can modify its physical and chemical properties, leading to an improved performance in various applications [13–15]. The activation of AC is known to play a key role

in enhancing adsorption efficiency via surface morphology modifications with certain functional groups [15–18].

Zeolites are three-dimensional aluminosilicate minerals with a porous structure that have valuable merits, such as cation exchange, molecular sieving, catalysis, and adsorption [19–21]. However, in many cases, these materials do not exhibit high adsorption efficiencies for target metals, and therefore their modification has been reported to enhance their adsorption potential [6, 21–23]. Chitosan, as an abundant natural polysaccharide, has attracted much attention in the biomaterial area because of its biocompatibility, biodegradability, and nonantigenicity [20, 21, 24]. Then, it is expected that the zeolite/chitosan hybrid material, which can incorporate the merits of both materials, may exhibit promising capability for the removal of heavy metal from aqueous solution.

Considering the above, adsorption experiments for heavy metals from aqueous solutions by modified carbon and zeolite/chitosan hybrid material were carried out using Inductively Coupled Plasma Atom Emission Spectrometer (ICP-AES) and ICP-MS in this work to obtain the optimum conditions for heavy metal adsorption process. In this paper, we first present the results of adsorption experiments for U(VI) using "Yukitsubaki" carbon (special product for Aga Town in Niigata Prefecture; abbreviated to YKC herein after) modified with nitric acid as part of the adsorption study of metals using relatively low-cost biomass. Second, the results of adsorption experiments for Pb by activated carbon modified with nitric acid are shown. Then, we finally present the results of adsorption experiments for Pb using zeolite/chitosan hybrid composite (abbreviated to ZCHC herein after).

Our aim was to investigate the efficiency of biomass (or the material prepared by biomass) as an adsorbent for heavy metals for more practical use in the future. Adsorption isotherms of heavy metals were studied and analyzed using Langmuir and Freundlich equations. Furthermore, to evaluate the characteristics of the adsorbents used in this work, the surface morphology, specific surface area, and functional groups of these materials were determined by SEM (Scanning Electron Microscopy), N_2-BET (Brunaeur, Emmet, and Teller) method, and FT-IR (Fourier Transform Infrared Spectroscopy).

2. Experimental Work

2.1. Samples

2.1.1. The charcoal (Yukitsubaki carbon, YKC) modified with nitric acid (HNO_3)

YKC was made from the trunk of *Camellia japonica L.*, which grows in the northeast of Japan, a particularly special product of Aga Town in Niigata Prefecture. YKC was pestled and sieved with 60 mesh. For the removal of ash in YKC, deashing was carried out with boiled ultrapure water. Then, it was dried at 110 °C in an oven. For enhancing the adsorption capacity, YKC carbon was oxidized in 10% HNO_3 and 30% HNO_3 at 90 °C for 4 h and washed with ultrapure water in order to completely remove the residue. Subsequently the sample was heated at 300

°C for 2 h to remove the residual nitrate ions on YKC. In this paper, the pristine YKC, and the modified YKCs oxidized by 10% and 30% HNO_3 were named YKC0, YKC10, and YKC30, respectively.

2.1.2. The Activated Carbon (AC) modified with potassium permanganate ($KMnO_4$)

Activated carbon was washed with deionized water (at 80 °C) to remove fine powders and contaminants, and was then dried at 110 °C for 2 h before use. Five grams of activated carbon was placed in a 200-mL conical flask, which contained 50 mL $KMnO_4$ solution (0.01 or 0.03 mol/L). After adjusting the temperature to 25 °C and stirring for 12 h, the resulting solution was filtrated through a 0.45-μm membrane filter. Then, the filtrate was washed with deionized water until the pH of the filtrate was constant. The activated carbon was dried at 70 °C for 6 h. The untreated and treated (i.e., modified with 0.01 mol/L and 0.03 mol/L $KMnO_4$ solution) activated carbon were described as AC_0, AC_{K1}, and AC_{K3}, respectively.

2.1.3. The Zeolite/Chitosan Hybrid material (ZCHC)

Zeolite was heated at 700 °C for 3 h to activate the surface in a muffle furnace and then washed with hydrochloric acid (5%, volume) and deionized water (at 80 °C) to remove fine powders and contaminants and was then dried at 110 °C for 2 h before use.

ZCHC was prepared by mixing solutions of chitosan and dispersions of zeolite in water. The general procedure of the synthesis is based on sol–gel method [25, 26]. First, 1 g chitosan was dissolved in 20 mL of 0.2 M acetic acid with constant stirring at temperature of 50 °C. Then, 10 mL of deionized water was added into 10 mL chitosan sol solution and was heated and stirred for 1 h. These solutions were mixed, while zeolite was dispersed in the chitosan solution with constant stirring for 5 h at a temperature of 50 °C. Then, the solution was transferred into five 10-mL centrifuge tubes, which were centrifuged at 9000 rpm for 5 min, and then washed with deionized water to remove contaminants. The mixed solutions were put on Petri dishes and were left to dry at room temperature for 24 h. The obtained films with a thickness of 0.1 mm were used for the following adsorption experiments.

2.2. Adsorption experiment for heavy metals using natural materials prepared by biomass

The following adsorption experiments were performed in a batch system using the above-mentioned samples. Experimental conditions (i.e., pH, contact time, sorbent amount, and temperature) in this work were optimized and determined based on our preliminary experiments and other studies [15, 20, 22]. The pH of each solution was adjusted by using 0.1 $molL^{-1}$ NH_3 aq/0.1 $molL^{-1}$ HNO_3. Adsorption isotherms of heavy metals onto these materials were measured at varying initial concentrations under optimized condition.

2.2.1. The charcoal (Yukitsubaki carbon, YKC) modified with nitric acid (HNO_3)

Each YKC sample of 30 mg was contacted with 50 mL of a known amount of U(VI) in a 100-mL conical flask, and the suspensions were shaken in a water bath. Adsorption experiments were conducted in the pH range of 2–10, with an adsorbent dosage of 0.1–0.6 gL^{-1}, at a

temperature of 5–45 °C, contact time from 1 to 24 h, and an initial concentration from 0 to 200 μgL^{-1}.

2.2.2. The Activated Carbon (AC) modified with potassium permanganate ($KMnO_4$)

Activated carbon was thoroughly mixed with 50 mL of a known amount of Pb^{2+} in a 200-mL conical flask, and the suspensions were shaken in a water bath at room temperature (25 ± 2 °C). Adsorption experiments were conducted in the pH range of 3–7, with an adsorbent dosage of 0.1–1.5 gL^{-1}, contact time from 1 to 24 h, and an initial concentration from 20 to 200 mgL^{-1}.

2.2.3. The zeolite/chitosan hybrid material (ZCHC)

Each ZCHC was thoroughly mixed with 50 mL of a known amount of Pb^{2+} in a 200-mL conical flask, and the suspensions were shaken in a water bath at room temperature (25 ± 2 °C). Adsorption experiments were conducted in the pH range of 3–7, a contact time from 1 to 48 h, and an initial concentration from 20 to 200 mgL^{-1}, with an adsorbent dosage of 1.0 gL^{-1}.

Following each sorption experiment, the suspension containing modified carbon (or ZCHC) and heavy metal solution was filtered through a 0.45-μm membrane filter (Advantec Mixed Cellulose Ester, 47 mm) to remove heavy metals that have been adsorbed into the adsorbent, and the concentration of these metals in the filtrate was determined with ICP-MS (X2, ThermoFisher) or AAS (Z-5000, HITACHI).

The metal uptake by each adsorbent was calculated using the following equation:

$$q = \frac{(C_i - C_e)}{m} \cdot V \tag{1}$$

where q is the adsorption capacity of heavy metal with the adsorbent at equilibrium (mg g^{-1}), C_i and C_e are the initial and equilibrium concentrations of heavy metal in a batch system, respectively (mg L^{-1}), V is the volume of the solution (L), and m is the weight of the adsorbent (g).

2.3. Langmuir and Freundlich isotherm model

Adsorption isotherms are commonly used to reflect the performance of adsorbents in adsorption processes. To examine the relationship between the metal uptake (q_e) and the concentration of metal ions (C_e) at equilibrium, adsorption isotherm models are widely used for fitting data.

The Langmuir model assumes monolayer adsorption on a surface given by the following equation:

$$\frac{C_e}{q_e} = \frac{C_e}{q_{max}} + \frac{1}{K_L q_{max}} \tag{2}$$

where C_e is the concentration of U(VI) (or Pb^{2+}) in a batch system at equilibrium (mg L^{-1}), q_e is the amount of U(VI) (or Pb^{2+}) adsorption at equilibrium (mg g^{-1}), q_{max} is the maximum adsorption capacity on the surface of activated carbon (or ZCHC) (mg g^{-1}), and K_L is the Langmuir adsorption constant (L mg^{-1}) [27, 28]. A plot of C_e/q_e versus C_e gives a straight line with a slope of $1/q_{max}$, and an intercept of $1/(K_L q_{max})$.

The Freundlich equation is widely used in the field of environmental engineering and was applied based on the work by Dahiya et al. [1, 29]. Freundlich isotherm can also be used to explain adsorption phenomenon as given below:

$$\log_{10} q_e = \log_{10} K_F + (1/n)\log_{10} C_f \tag{3}$$

where K_F and n are constants incorporating all factors affecting the adsorption capacity and an indication of the favorability of metal ion adsorption onto a biosorbent, respectively. It is shown that $1/n$ values between 0.1 and 1.0 correspond to beneficial adsorption. That is, q_e versus C_f in a log scale can be plotted to determine the values of $1/n$ and K_F.

2.4. Kinetic model

Kinetics of heavy metal uptake was modeled using the pseudo-first-order and pseudo-second-order Lagergren equations [30, 31]. The pseudo-first-order reaction of Lagergren for sorption can be expressed as follows based on Bhat et al. [32]:

$$dQ/dt = k_1(Qe - Qt) \tag{4}$$

where Qe and Qt are the amount of metal adsorbed per unit weight (μg/g) of sorbent at equilibrium and at any time t (min), respectively, and k_1 is the rate constant of pseudo-first-order sorption (min^{-1}). The integrated form of the above equation after applying the boundary conditions, for $t = 0$, $qt = 0$, becomes

$$\log(Qe - Qt) = \log(Qe) - (k_1/2.303)t \tag{5}$$

The value of the rate constant (k_1) and Qe for the pseudo-first-order sorption reaction can be obtained by plotting log(Qe −Qt) versus t.

The pseudo-second-order rate of Lagergren can be expressed as follows:

$$DQ/dt = k_2(Qe - Qt)^2 \tag{6}$$

where k_2 (g/(μg min)) is the rate constant for the pseudo-second-order sorption. The integrated linear form of Eq. (9) can be represented as follows:

$$t / Q = 1 / k_2 Q^2{}_e + (1 / Q_e)t \tag{7}$$

The pseudo-second-order rate constant (k_2) and Q_e can be calculated from the intercept and slope of the linear plot of t/Qt versus t.

The initial adsorption rate (h) can be determined from k_2 and Qe values using

$$h = k_2 Q\mathrm{e}^2 \tag{8}$$

3. Results and discussion

3.1. The charcoal (Yukitsubaki carbon, YKC) modified with nitric acid (HNO_3)

3.1.1. Characterization of YKC

The morphologies of pristine and modified YKCs characterized by SEM (JCM-6000, JEOL) are shown in Figure 1. Moreover, the surface properties including specific surface areas of pristine and modified YKCs determined by N_2-BET method (TriStar II 3020, Micromeritics) are shown in Table 1. The pore structures of all the samples are similar to each other. However, judging from the SEM image shown in Figure 1, the surface area of YKC30 (Figure 1C) seems to be slightly changed with the acid treatment, whereas that of YKC10 (Figure 1B) seems to be hardly varied. This is consistent with the data of the specific surface area shown in Table 1. The decrease in the specific surface area of YKC30 would be attributable to the excessive oxidation with a high concentration of nitric acid.

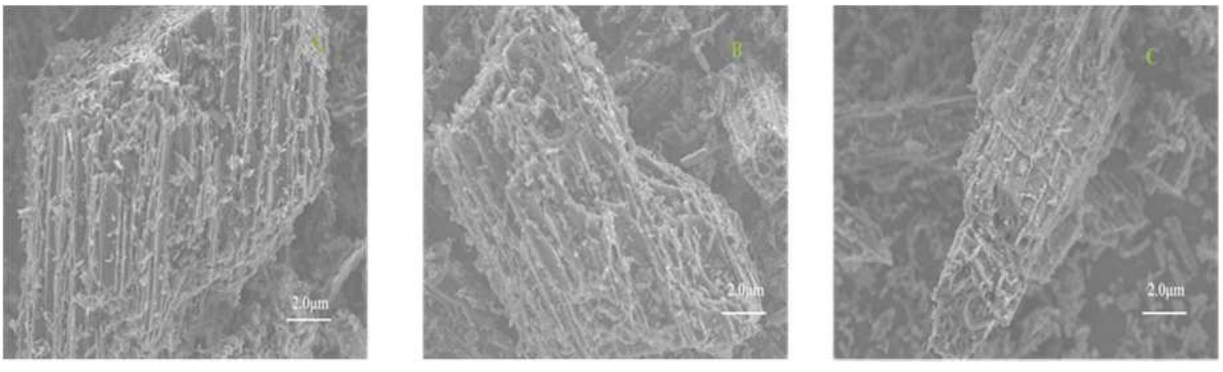

Figure 1. The SEM images of pristine and modified YKCs. (A: YKC0, B: YKC10, C: YKC30)

The FT-IR (FTIR-4200, Jasco) spectra of pristine and modified YKCs are shown in Figure 2. From the figure, a characteristic broadband, which may be due to graphite structure in YKCs,

http://dx.doi.org/10.5772/61507

Samples	Specific surface area (m^2/g)	Pore volume (cm^3/g)	Pore size (nm)
YKC0	157	0.0854	2.18
YKC10	158	0.0852	2.16
YKC30	144	0.0774	2.15

Table 1. Surface properties of pristine and modified YKCs

is observed at around 1610 cm^{-1}. The peak at 3300 cm^{-1} is related to hydroxyl groups (–OH), and 1120 cm^{-1} is related to carbonyl groups (–C=O), and then the peaks at 2920 and 2850 cm^{-1} are associated with C–H [33–36]. The results of FT-IR analysis show that some kinds of functional groups (such as carbonyl groups and hydroxyl groups) are introduced to YKC surfaces successfully by oxidation.

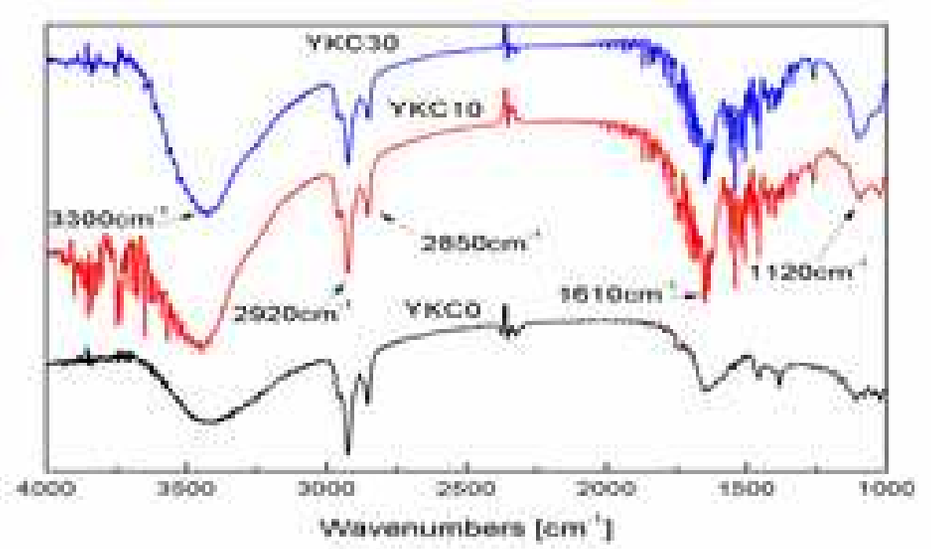

Figure 2. The FT-IR spectra of pristine and modified YKCs

3.1.2. Influence of parameters on adsorption

3.1.2.1. Contact time

The effect of contact time on U(VI) adsorption was investigated to study the adsorption rate of U(VI) removal. The percentage removal of U(VI) for the concentration of 100 μg/L with the adsorbent dosage of 30 mg at a pH of 3.0 is shown in Figure 3.

The adsorption equilibrium of U(VI) on YKC10 was reached within 30 min, much faster than that on YKC0 and YKC30. For the rest of the study, 480 min (8 h) was selected as the contact time.

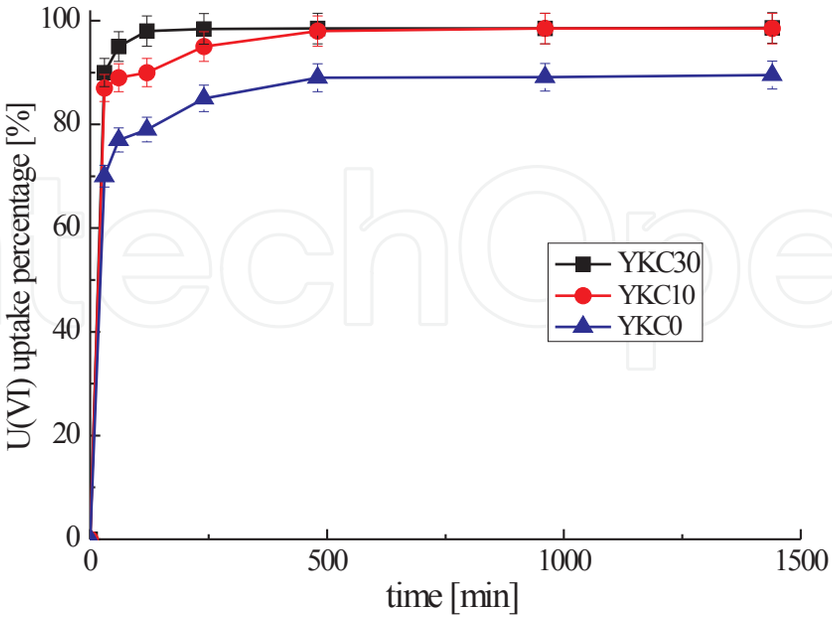

Figure 3. Effect of contact time on U(VI) adsorption (pH = 3.0, T = 25 °C, and adsorbent dose of 30 mg)

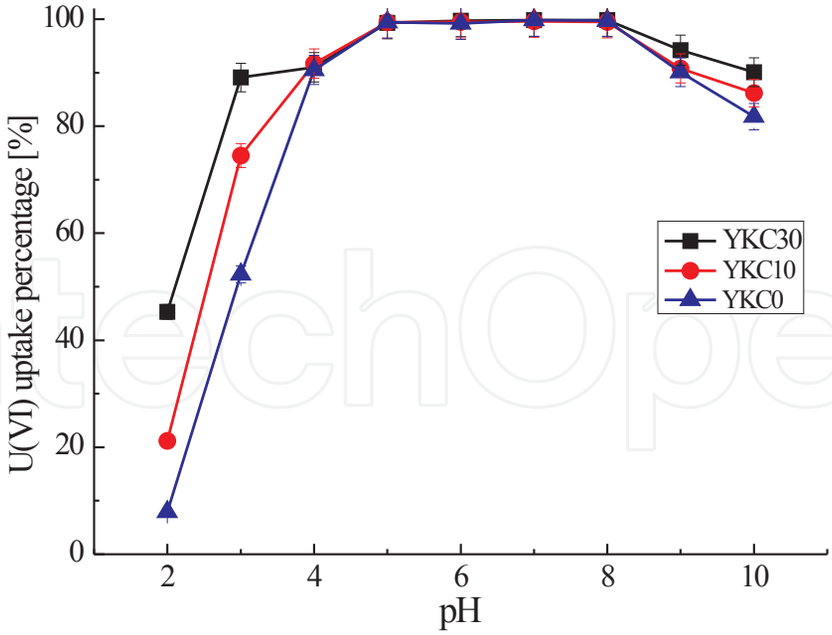

Figure 4. Effect of pH on U(VI) adsorption (contact time of 8 h, T = 25 °C, and adsorbent dose of 30 mg)

The adsorption of U(VI) on the YKC as a function of pH is shown in Figure 4. From this figure, it can be seen that the amount of U(VI) uptake increased with increasing solution pH. The highest uptake was observed at a pH of 5–8 for all YKCs, and the uptake of U(VI) decreased slightly with increasing pH at a pH of >8. The difference in the pH dependence is not clearly found among YKCs, although the difference of adsorption capacities among YKCs was obviously found. It is known that U exists in different forms depending on the pH. U exists predominantly as monomeric species UO_2^{2+}, and small amounts of UO_2 $(OH)^+$ at a pH of ≤4.3, and at a pH of ≥5, colloidal or oligomeric species, i.e., $(UO_2)_2(OH)_2^{2+}$, $(UO_2)_3(OH)_5^+$, $(UO_2)_4(OH)_7^+$, and $(UO_2)_3(OH)_7^-$, are formed [37–40].

That is, U usually exists as cationic species in solution at a pH of 5. Furthermore, from the results of the FT-IR spectra of YKC shown in Figure 2, hydroxyl groups (−OH) are introduced onto YKC.

From the above, it can be considered that the U(VI) adsorption occurred dominantly by the cation exchange reaction between the H^+ of hydroxyl groups on YKC and the cationic species of U(VI).

Then, a pH of 5 was assumed for further experimental work, although the uptake of U(VI) maintains the highest level at a pH of 5–8.

3.1.2.2. Adsorbent amount and adsorption temperature

Under optimized conditions of pH (i.e., pH 5) and contact time (i.e., 8 h), the adsorption behavior at different adsorbent amounts (10–60 mg) or adsorption temperatures (5–45°C) has been studied in 50 mL of a 100-μg/L aqueous U(VI) solution in 100-mL flasks.

From the above experiment, the adsorbent amount was selected as 30 mg in our work in consideration of the economic cost, although the adsorption efficiency slightly increased with an increase in the adsorbent amount. On the other hand, 25 °C was selected because the highest uptake was observed at 25 °C, and there is no appreciable change in the uptake of U(VI) with increasing temperatures.

3.1.3. Adsorption isotherm study

The Langmuir and Freundlich isotherms for the adsorption of U(VI) onto YKC are given in Figures 5 and 6.

The linear correlation coefficients (R^2) of Langmuir and Freundlich isotherms for U(VI) using pristine and modified YKCs are shown in Table 2 along with other parameters.

From this table, it is found that the R^2 value for each datum is comparatively large for both Langmuir and Freundlich isotherms. Furthermore, it is noted that R^2 values for these data are larger for the Langmuir isotherm than for the Freundlich isotherm. This result suggests that the adsorption on these samples mainly occurred by a monolayer reaction.

From the data of Q_m in Table 2, it is also found that the adsorption capacity of U(VI) on modified YKC is much higher than that on pristine YKC. The results indicated that acid treatment is effective for enhancing the adsorption capacity of U(VI).

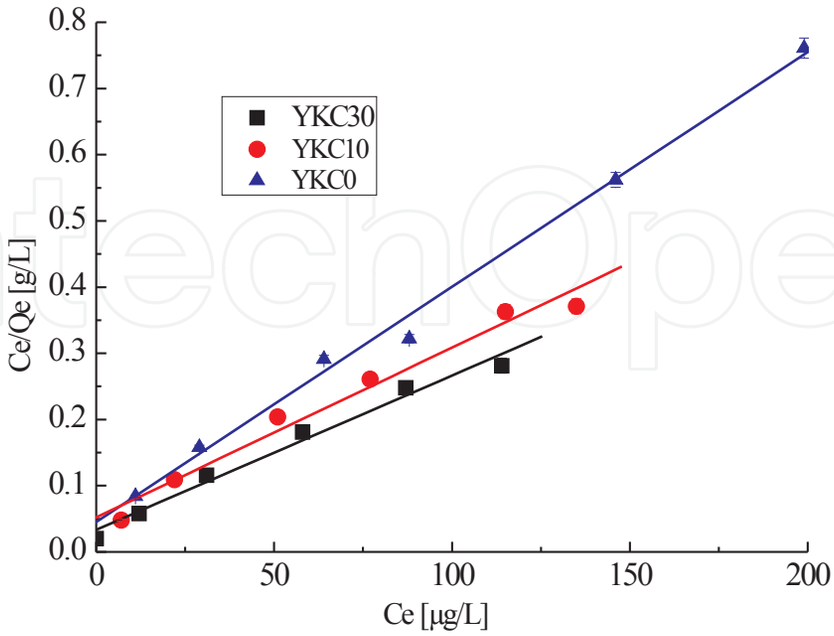

Figure 5. The Langmuir isotherm of U(VI) adsorption (pH = 5.0, T = 25 °C, and adsorbent dose of 30 mg)

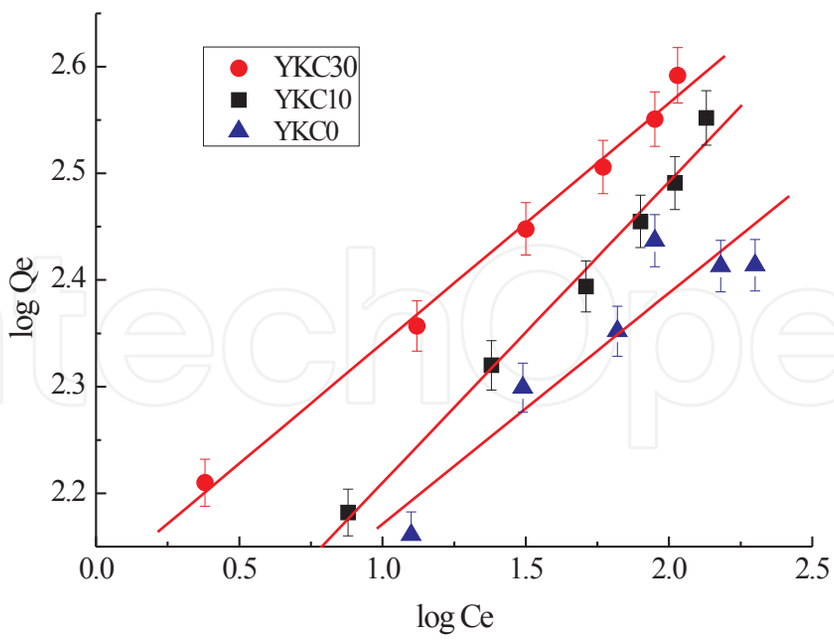

Figure 6. The Freundlich isotherm of U(VI) adsorption (pH = 5.0, T = 25 °C, and adsorbent dose of 30 mg)

http://dx.doi.org/10.5772/61507

	Langmuir isotherm			Freundlich isotherm		
	Q_m(μg/g)	K_L (L/μg)	R^2	b_F	K_F (μg/g)	R^2
YKC0	270	0.112	0.996	0.196	99.4	0.912
YKC10	417	0.0931	0.984	0.222	132	0.891
YKC30	385	0.0522	0.976	0.274	88.3	0.843

Table 2. Coefficients of Langmuir and Freundlich isotherm models

Here, Q_m is the maximum adsorption capacity of the U(VI) (μg/g), K_L is the Langmuir binding constant, which is related to the energy of adsorption (L/μg), and K_F and b_F are the Freundlich constants related to the adsorption capacity and intensity.

3.2. The activated carbon modified with potassium permanganate ($KMnO_4$)

3.2.1. Characterization of the modified activated carbon

The FT-IR spectra of the pristine and modified activated carbon (i.e., AC_0, AC_{K1}, and AC_{K3}) are shown in Figure 7. The pristine and modified activated carbon displayed the characteristic bands of the graphite structure of carbon at 1615 cm^{-1} [8, 15, 41]. Moreover, an OH stretching band, one of the typical peaks of activated carbon, was found at 3300–3500 cm^{-1}. The peak at 3433 cm^{-1} was related to the hydroxyl groups (−OH) stretch from deprotonated pristine and modified activated carbon. The wide peak at 1550–1750 cm^{-1} shows the asymmetric stretch of the carboxylate (−COO−) group [15].

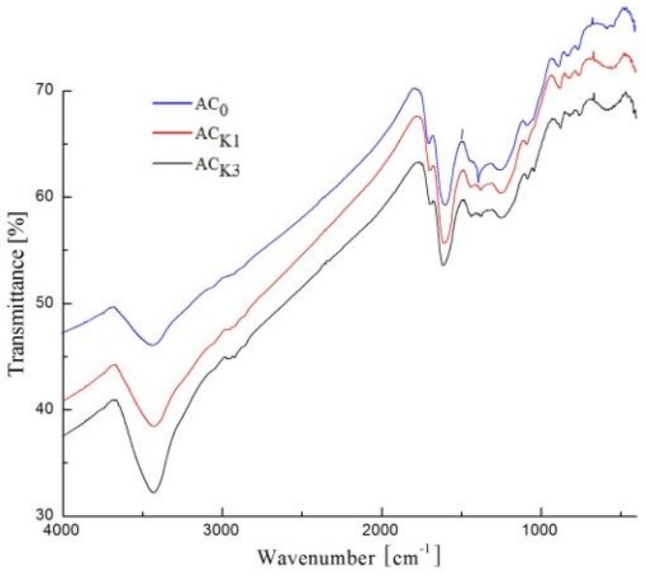

Figure 7. FT-IR spectra of AC_0, AC_{K1}, and AC_{K3}.

The surface properties of the activated carbon were investigated by N_2 adsorption (TriStar II 3020 Micromeritics), and the analytical results for the adsorption/desorption isotherms are shown in Table 3.

Adsorbent	BET surface area ($m^2 \cdot g^{-1}$)	Pore volume ($cm^3 \cdot g^{-1}$)	Pore size (nm)
AC_0	381	0.402	4.23
AC_{K1}	373	0.390	4.18
AC_{K3}	346	0.348	4.03

Table 3. Textural characteristics of activated carbon

The pore volume was calculated from the amount of N_2 adsorbed at the relative pressure of 0.99. The pore size was calculated from the adsorption average pore width (4V/A by BET) in this work. From Table 3, it is found that the pore volume and pore size as well as the specific surface area decreased significantly after modification with $KMnO_4$. The isotherm showed a type H1 isotherm with a clear hysteretic loop, characteristic of disordered microporous materials.

The SEM micrographs of the activated carbon are shown in Figure 8. The modified AC (Figures 8B and 8C) seemed to exhibit a more compact stacking morphology than the pristine AC (Figure 8A), due to cohesive forces, which may be generated from the introduction of oxygen-containing functional groups. These results are consistent with those of the N_2 adsorption–desorption experiment. The decrease of the pore volume and pore size may be related to the increase of acidic groups on the surface of activated carbon treated with $KMnO_4$.

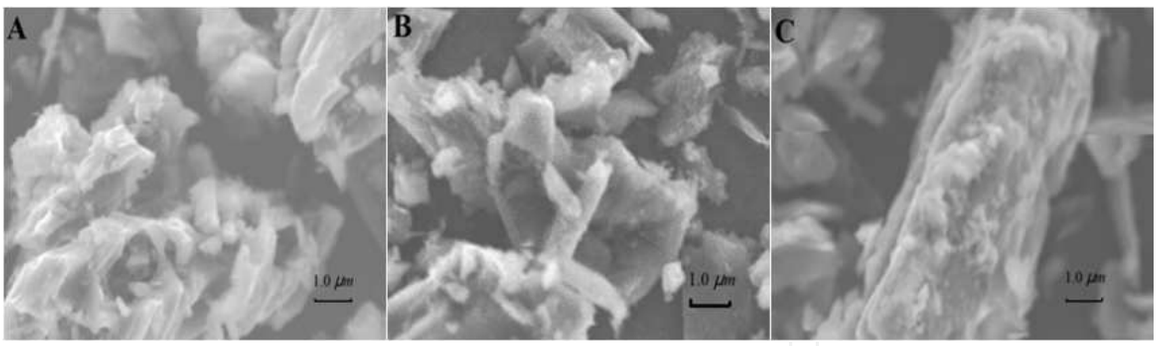

Figure 8. SEM micrographs of the surface of activated carbon: (A) unmodified; (B) modified with 0.01 mol/L $KMnO_4$; (C) modified with 0.03 mol/L $KMnO_4$

3.2.2. Adsorption of lead on modified activated carbon

3.2.2.1. Effect of pH

To investigate the effect of solution pH on Pb^{2+} adsorption efficiency, the pH of the solution was varied from 3 to 7, while the Pb^{2+} concentration was kept constant at 100 mg L^{-1}. The

http://dx.doi.org/10.5772/61507

experimental results are presented in Figure 9. The Pb^{2+} adsorption efficiency was at pH 5 regardless of the kind of adsorbent (Figure 9). The uptake of Pb^{2+} increased from 50.8% at pH 3 to 90.0% at pH 5, and at higher pH values, it remained almost constant (or decreased only slightly). Notably, the adsorption capacities decreased at low pH values due to the competition of protons with metal ions for active binding. On the other hand, lead precipitated from the solution at higher pH values as lead hydroxide [1]. From the FT-IR spectra of AC (Figure 7), it was clear that the hydroxyl groups (−OH) were introduced onto AC. We hypothesized that the Pb^{2+} adsorption occurred predominantly by cation exchange reaction between the H^+ of the hydroxyl groups on modified AC and cationic Pb^{2+} species. However, it is possible that Pb^{2+} was removed to some extent via precipitation at higher pH values rather than by adsorption on the modified AC. Hence, pH 5 was used for further experiments.

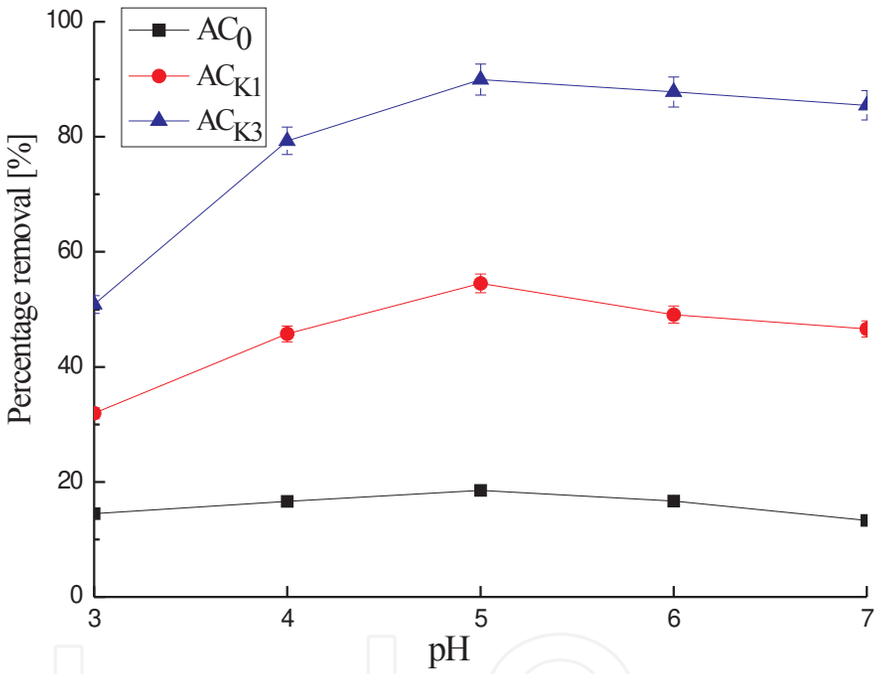

Figure 9. Effect of pH on the removal of Pb^{2+} (%) using modified activated carbon.

3.2.2.2. Effect of contact time

The effect of contact time on Pb^{2+} adsorption efficiency using 1.0 gL^{-1} AC_{K3} (100 mgL^{-1} of solution) was investigated at pH 5.

More than 80% Pb was removed within 1 h, and it gradually increased at 2 h. Approximately 90% of Pb was removed from the solution at the contact time of 2 h. After 2 h, there was no appreciable change. Therefore, 2 h was chosen as the optimized contact time for the rest of the experimental work.

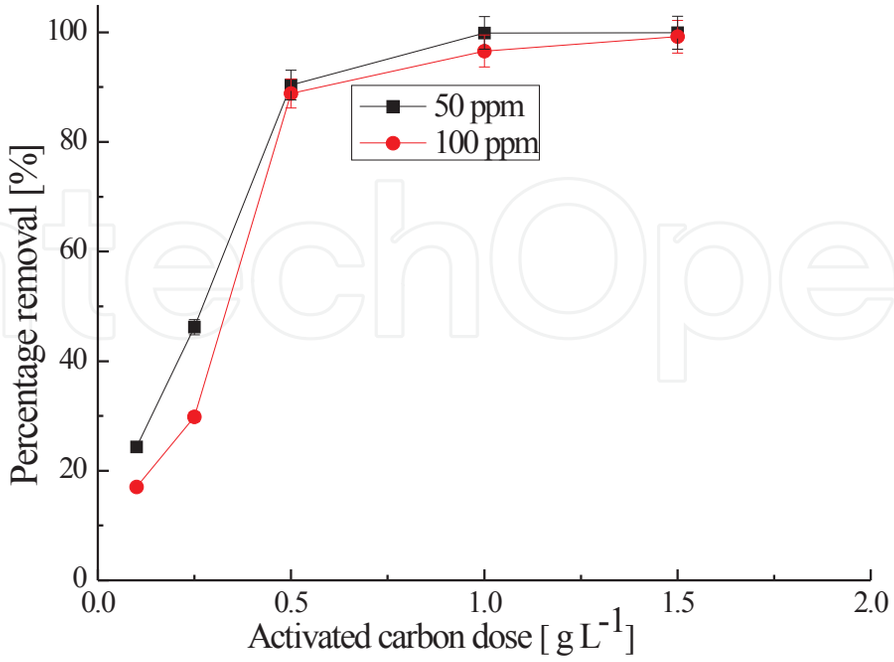

Figure 10. Effect of sorbent dosage on percent removal of Pb^{2+} using modified activated carbon

3.2.2.3. Effect of sorbent dosage

Under the optimized pH conditions (i.e., pH 5) and contact time (i.e., 2 h), the adsorption behavior of AC_{K3} at different dosages (from 0.1 to 1.5 gL^{-1}) was studied in 100 mgL^{-1} Pb^{2+} solution.

More than 90% of Pb^{2+} was removed with a dosage of 1.0 gL^{-1} (Figure 10). The removal increased remarkably with higher dosage rates, but no remarkable increase was observed at dosages greater than 1.0 gL^{-1}. Therefore, 1.0 gL^{-1} was considered as the optimum dosage for the remainder of the study.

3.2.2.4. Effect of competitive ions

Competitive experiments were conducted under the optimized pH conditions (i.e., pH 5), contact time (i.e., time 2 h), and sorbent dosage (i.e., 1 g/L) using different concentrations of Na^+, K^+, Ca^{2+}, or Mg^{2+} separately and combination of all four ions (i.e., 0, 10, 20, 50, 100, 200, and 500 mgL^{-1}). The percent removal of Pb^{2+} decreased in the presence of Na^+, K^+, Ca^{2+}, or Mg^{2+} with concentrations from 0 to 500 mgL^{-1} (Figure 11). A remarkable decrease in the adsorption capacity of Pb^{2+} was not observed, even with common ions at concentrations of 100 mgL^{-1} (i.e., more than 80% Pb^{2+} was removed; Figure 5). This implied that the activated carbon was an efficient adsorbent for Pb^{2+}, although further investigations are required for the realization of practical application.

http://dx.doi.org/10.5772/61507

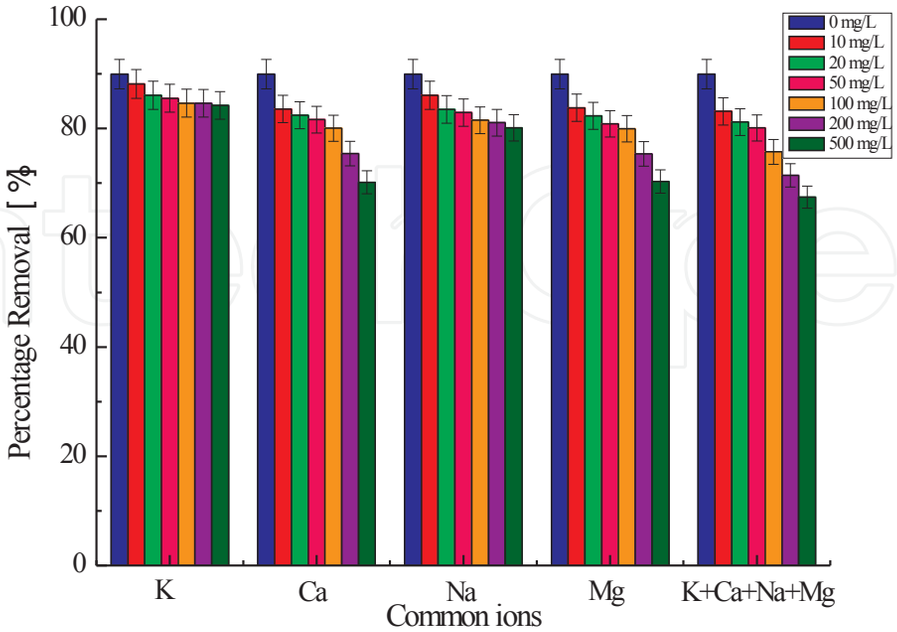

Figure 11. Effect of competitive ions on percent removal of Pb^{2+} using modified activated carbon.

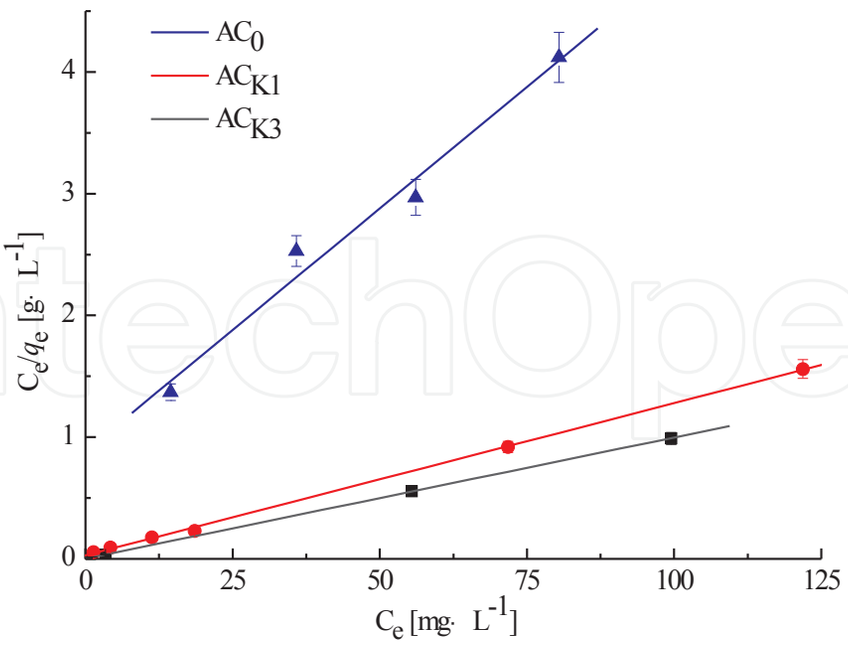

Figure 12. Langmuir isotherm of Pb^{2+} adsorption on AC.

3.2.3. Adsorption isotherms

Adsorption isotherms are commonly used to reflect the performance of adsorbents in adsorption processes. The Langmuir adsorption isotherm was applied to the data obtained in this work. A plot of C_e/q_e versus C_e based on the Langmuir model is shown in Figure 12.

From these data, the q_{max} and K_L of AC_0, AC_{K1}, and AC_{K3} were calculated and are shown in Table 4 along with the R^2 (correlation coefficient). The adsorption capacity of AC modified with 0.03 mol/L $KMnO_4$ was about 4 times higher than that of pristine AC.

Adsorbent	q_{max} ($mg \cdot g^{-1}$)	KL ($L \cdot mg^{-1}$)	R
AC_0	25.1	0.0452	0.983
AC_{K1}	80.0	0.435	0.998
AC_{K3}	101	4.60	1.00

q_{max}: the maximum adsorption capacity on the surface of activated carbon (mg g^{-1});

K_L: the Langmuir adsorption constant (L mg^{-1});

R: the correlation coefficient.

Table 4. Coefficient of Langmuir isotherm for Pb^{2+} using AC

The R^2 value for each adsorbent was comparatively large (Table 4). Furthermore, the R^2 value for modified AC (i.e., AC_{K1} and AC_{K3}) was particularly large. That is to say, a favorable adsorption of Pb^{2+} by activated carbon was apparent. This result suggested that the adsorption of these samples primarily occurred via a monolayer reaction.

Biosorbent	Maximum adsorption capacity ($mg \cdot g^{-1}$)	Reference
Acidified MWCNTs	49.7	[42]
Cicer arientinum biomass	27.8	[7]
Sawdust of Meranti wood	37.2	[43]
Activated carbon prepared from apricot stone	22.9	[16]
Peanut husks carbon	70.0	[44]
Activated carbon modified with KMnO4	101	Present study

Table 5. Comparison of Pb^{2+}adsorption capacities of modified AC with other adsorbents

Next, the adsorption capacity of Pb^{2+} by modified AC was compared with other adsorbents under ambient conditions previously reported in the literature. As shown in Table 5, the

http://dx.doi.org/10.5772/61507

maximum adsorption capacity of modified AC toward Pb^{2+} was higher than that of other adsorbents.

The adsorption capacity of activated carbon may be dependent on its surface properties ([7], [45]). Therefore, the modification with $KMnO_4$ (an efficient oxidizer) could change the surface structure of activated carbon to enhance the adsorption capacity of AC toward metals.

3.2.4. Kinetic studies

The linear plot of t/q_t versus t for metal adsorption under the optimized experimental conditions is shown in Figure 13. The coefficient of determination was more than 0.996 of Pb^{2+} on modified AC. The pseudo-second-order rate constant (k) and the amount of adsorbed lead (q_e) obtained from the intercept and slope of the plot of t/q_t versus t are listed in Table 6 along with the regression coefficient (R^2).

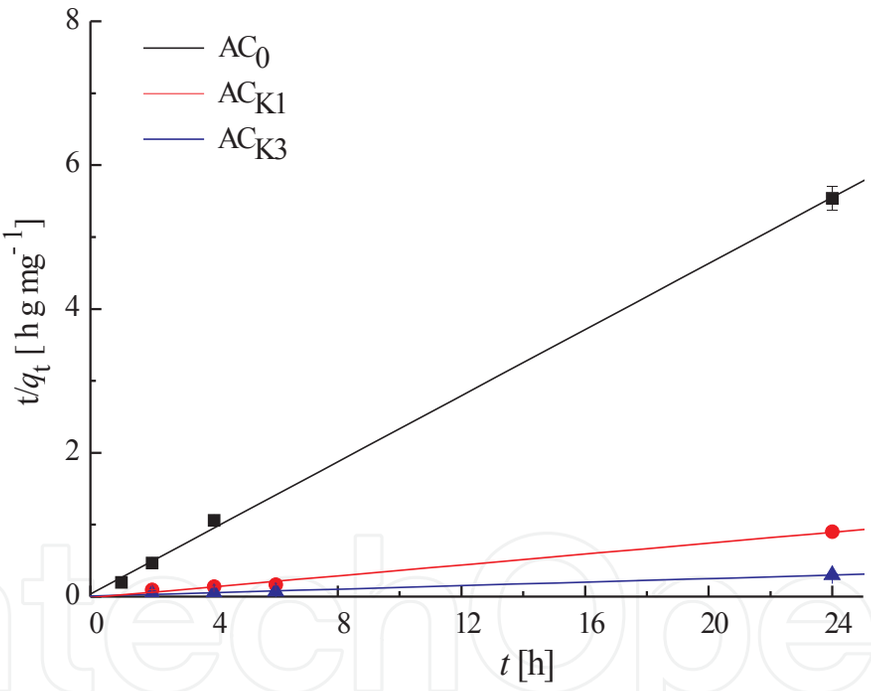

Figure 13. The pseudo-second-order kinetic model for AC.

The adsorption kinetics based on the experimental values were in good agreement with the pseudo-second-order kinetic model. The intraparticle diffusion model indicated that the relationship between the concentration of Pb^{2+} and the square root of time was linear. This suggested that the adsorption process could be controlled by intraparticle diffusion. Moreover, the adsorption at higher temperatures became more dependent on intraparticle diffusion, the rate-determining step.

Activated carbon	*qe* (mg·g^{-1})	*k* (g·mol^{-1}·h^{-1})	*R*
AC_0	26.4	2.87×10^{-3}	0.999
AC_{K1}	81.8	1.16×10^{-2}	0.999
AC_{K3}	101	4.51×10^{-2}	0.999

q_e: the amount of adsorbed lead on the surface of activated carbon at equilibrium (mg g^{-1});

k : the rate constant of the pseudo-second-order adsorption (g mol^{-1} h^{-1});

R: the correlation coefficient.

Table 6. Kinetic coefficients for Pb^{2+} adsorption on AC

3.3. The zeolite/chitosan hybrid material (ZCHC)

3.3.1. Characterization of ZCHC

The surface properties of ZCHC before and after Pb^{2+} adsorption were investigated by N_2 adsorption (TriStar II 3020, Micromeritics), and the analytical results for the adsorption/desorption isotherms are shown in Table 7.

Adsorbent	BET surface area (m^2·g^{-1})	Pore volume (cm^3·g^{-1})	Pore size (nm)
ZCHC (before adsorption)	9.25	0.0485	21.0
ZCHC (after adsorption)	9.19	0.0479	20.7

Table 7. Textural characteristics of ZCHC

The pore volume was calculated from the amount of N_2 adsorbed at the relative pressure of 0.99. The pore size was calculated from the adsorption average pore width (4V/A by BET) in this work.

The SEM micrographs of the ZCHC before and after Pb^{2+} adsorption ZCHC are shown in Figure 14. From Figure 14, it is found that the morphology of ZCHC surface has hardly changed even after exposing Pb^{2+}, although the SEM picture after Pb^{2+} adsorption slightly exhibits a more compact stacking morphology than that before adsorption. From the above observation, ZCHC should be predicted to withstand the repeated use, and hence it can be a good adsorbent for heavy metals such as Pb^{2+}. These results are consistent with those of the N_2 adsorption–desorption experiment.

http://dx.doi.org/10.5772/61507

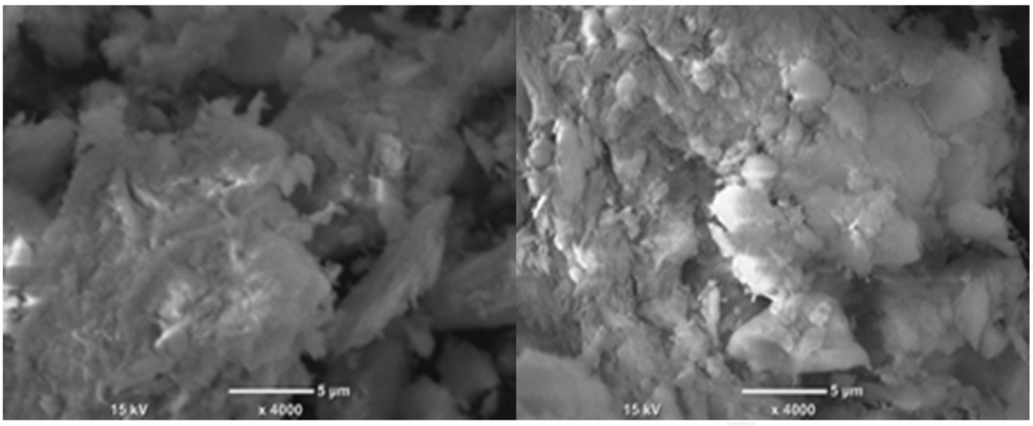

(A) (B)

Figure 14. SEM micrographs of the surface of ZCHC: (A) before Pb^{2+} adsorption; (B) after Pb^{2+} adsorption.

3.3.2. Adsorption of lead on zeolite and ZCHC

With the aim of obtaining the optimum conditions, the effects of pH value and contact time in the case of a fixed dosage of adsorbent (i.e., 1.0 g L^{-1}) on the removal of Pb^{2+} from the aqueous solution were investigated. The effect of pH on Pb^{2+} adsorption onto zeolite and ZCHC is shown in Figure 15. From Figure 15, the uptake of Pb^{2+} increased from 56.7% at pH 3 to 95.6% at pH 5, and at higher pH value, it remained almost constant (or decreased slightly). Notably, the adsorption capacities decreased at low pH values due to the competition of protons with metal ions for active binding. On the other hand, lead precipitated from the solution at higher pH values as lead hydroxide. Hence, pH 5 was used for further experiments.

The effect of contact time on Pb^{2+} adsorption onto zeolite and ZCHC is shown in Figure 16. Approximately 90% of Pb was removed from the solution with ZCHC at the contact time of 1 h, and it gradually increased at 4 h as shown in Figure 16. More than 95% of Pb was removed from the solution at the contact time of 4 h. After 4 h, there was no appreciable change. On the other hand, a contact time of 8 h was needed to attain at equilibrium in case of zeolite. Therefore, 8 h was chosen as the optimized contact time for more certainty for these samples at the rest of the experimental work.

3.3.3. Adsorption isotherms

Adsorption isotherms are commonly used to reflect the performance of adsorbents in adsorption processes. The Langmuir adsorption isotherm was applied to the data obtained in this work. A plot of C_e/q_e versus C_e based on the Langmuir model is shown in Figure 17.

As shown in Table 8, R value for each adsorbent was comparatively large, and a favorable adsorption of Pb^{2+} by these samples was apparent. This result suggested that the adsorption of these samples primarily occurred via a monolayer reaction. Furthermore, the maximum adsorption capacity of ZCHC toward Pb^{2+} was higher than that of zeolite.

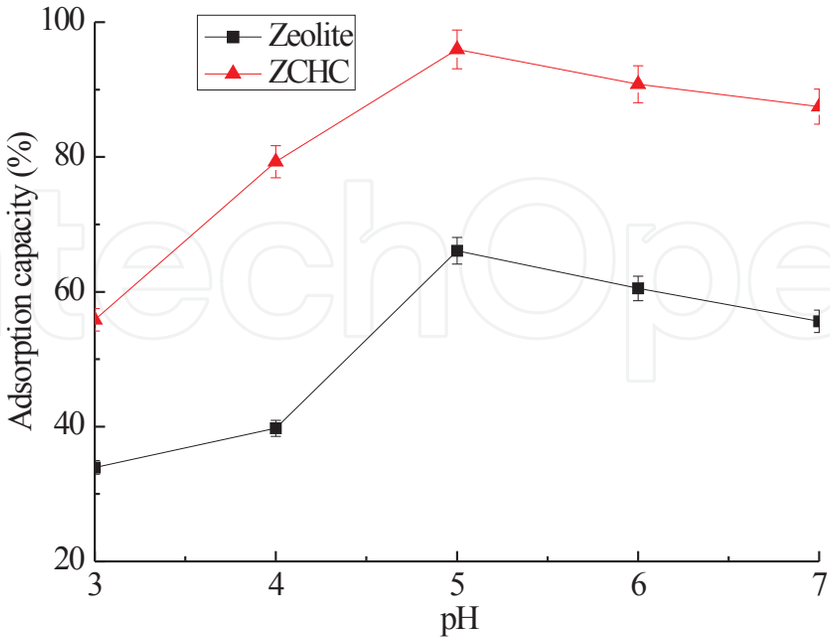

Figure 15. Effect of pH on the removal of Pb^{2+} removal of using zeolite and ZCHC. Pb^{2+} using zeolite and ZCHC.

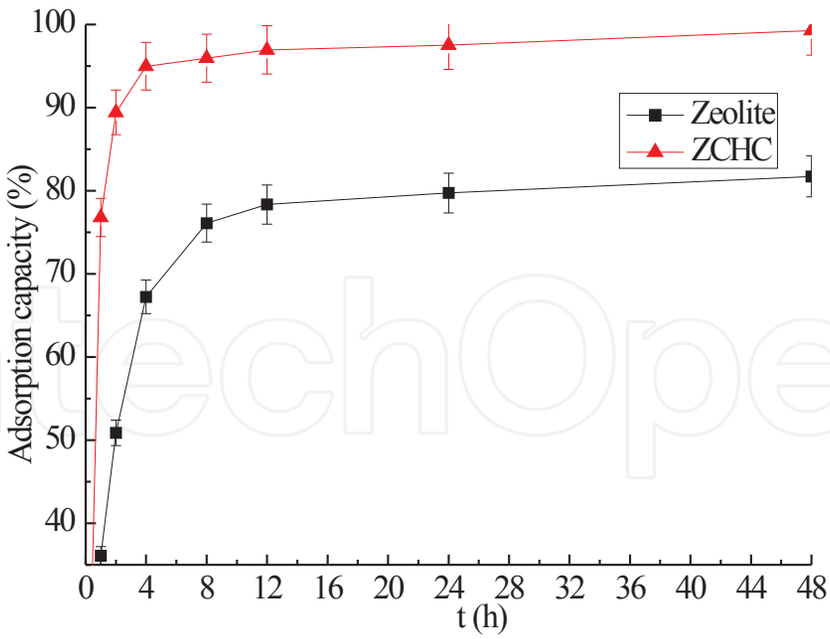

Figure 16. Effect of contact time on the

http://dx.doi.org/10.5772/61507

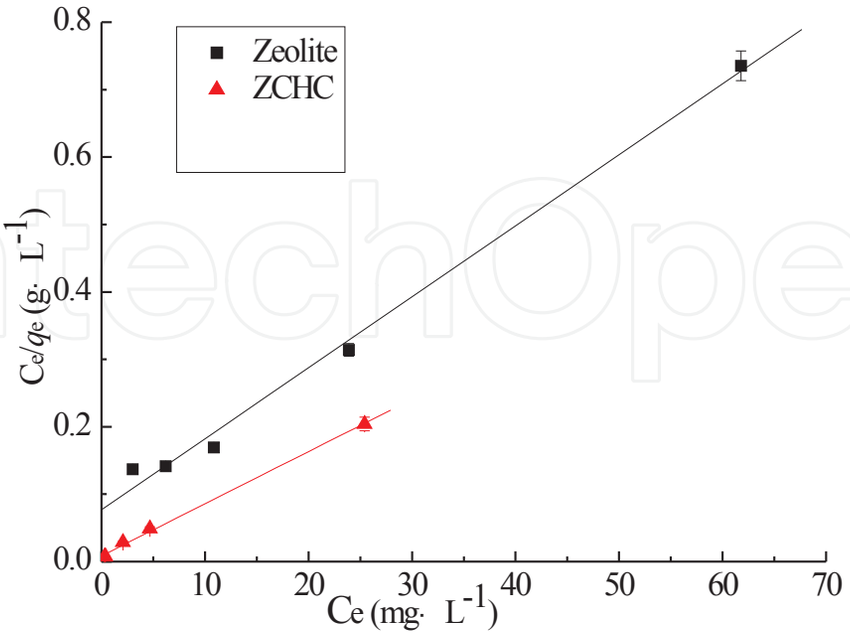

Figure 17. Langmuir isotherm of Pb^{2+} adsorption on zeolite and ZCHC.

Adsorbent	q_{max} ($mg \cdot g^{-1}$)	*KL* ($L \cdot mg^{-1}$)	*R*
Zeolite	66.5	0.196	0.997
ZCHC	139	0.844	0.999

q_{max}: the maximum adsorption capacity (mg g^{-1});

K_L: the Langmuir adsorption constant (L mg^{-1});

R: the correlation coefficient.

Table 8. Coefficient of Langmuir isotherm for Pb^{2+} using zeolite and ZCHC

4. Conclusion

Yukitsubaki carbon (charcoal) modified with nitric acid (10% and 30%), activated carbon modified with potassium permanganate ($KMnO_4$; 0.01 mol/L and 0.03 mol/L), and zeolite/chitosan hybrid composite (ZCHC) prepared with sol–gel method were used as adsorbents for heavy metal ions in this work. Modified carbon treated with HNO_3 or $KMnO_4$ exhibits high ability of chemical adsorption and stronger chemical affinity than pristine carbon. ZCHC prepared in this work also could be suitable as sorbent materials for the removal of heavy metals from aqueous solutions. The adsorbent showed excellent adsorption capacity for Pb^{2+} under our experimental condition, even in the presence of diverse ions (Ca^{2+}, Mg^{2+}, Na^{+}, and

K^+) up to the concentration of 100 $mgdm^{-3}$. It is indicated that these materials used in this work could be effective adsorbents for practical use in the future.

It is also suggested that the removal of U and Pb from aqueous solutions by these materials is mainly due to monolayer sorption because of well fitting for Langmuir model. Furthermore, the best fit was obtained with a pseudo-second-order kinetic model while investigating the adsorption kinetic of carbon modified with HNO_3 or $KMnO_4$.

The data obtained and the method used in this work can be a useful tool from the viewpoint of environmental protection and resource recovery in future work.

Acknowledgements

The present work was partially supported by a Grant-in-Aid for Scientific Research (Research Program (C), No. 25340083) of the Japan Society for the Promotion of Science. This research was also supported by a fund for the promotion of Niigata University KAAB Projects from the Ministry of Education, Culture, Sports, Science and Technology, Japan.

The present work was partially supported by a Grant-in-Aid for Scientific Research of the Japan Society for the Promotion of Science. Yukitsubaki carbon samples were supplied by Mr. J. Sakai of the Facility of Engineering in Niigata University. The authors are also grateful to Mr. N. Saito, Mr. T. Nomoto, Prof. T. Tanaka, Mr. T. Hatamachi, Dr. M. Teraguchi and Prof. T. Aoki of the Facility of Engineering in Niigata University for permitting the use of SEM, Surface Area Analyzer, and FT-IR, and thanks to Dr. K. Fujii and Mr. M. Ohizumi of the Office for Environment and Safety in Niigata University for permitting the use of ICP-MS and for providing helpful advice in measurement.

Author details

Naoki Kano*

Address all correspondence to: kano@eng.niigata-u.ac.jp

Department of Chemistry and Chemical Engineering, Faculty of Engineering, Niigata University, Nishi-Ku, Niigata, Japan

References

[1] Dahiya S., Tripathi R. M., Hegde A. G. (2008) Biosorption of Heavy Metals and Radionuclide from Aqueous Solutions by Pre-treated Arca Shell Biomass. J. Hazard. Mater., 150: 376–386.

[2] Sachdeva S., Kumar A. (2009) Preparation of nanoporous composite carbon membrane for separation of rhodamine B dye. J. Membr. Sci., 329: 2–10.

[3] Wang J., Chen C. (2009) Biosorbents for heavy metals removal and their future. Biotechnol. Adv., 27: 195–226.

[4] Shashikant R.M., Rajamanya V. S. (2003) Biosorption studies of chromium and pentachlorophenol from tannery effluents. Bioresour. Technol., 98: 1128–1132.

[5] Pillai S. S., Mullassery D. M., Fernandez B. N., Girija N., Geetha P., Koshy M. (2013) Biosorption of Cr(◎) from aqueous solution by chemically studies. Ecotoxicol. Environ. Saf.., 92: 199–205.

[6] Repo E., Warchol J. K., Bhatnagar A., Sillanpaa M. (2011) Heavy metals adsorption by novel EDTA-modified chitosan-silica hybrid materials. J. Colloid Interface Sci., 358: 261–267.

[7] Ren X., Chen C., Nagatsu M., Wang X. (2011) Carbon nanotubes as adsorbents in environmental pollution management: A review. Chem. Eng. J., 170: 395–410.

[8] Zhu J., Yang J., Deng B. (2010) Ethylenediamine-modified activated carbon for aqueous lead adsorption. Environ. Chem. Lett., 8: 277–282.

[9] Mellah A., Chegrouche S., Barkat M. (2006) The removal of uranium(VI) from aqueous solutions onto activated carbon kinetic and thermodynamic investigations. J. Colloid Interface Sci., 296: 434–441.

[10] Kumar S., Loganathan V. A., Gupta R. B., Barnett M. O. (2011) An assessment of U(VI) removal from groundwater using biochar produced from hydrothermal carbonization. J. Environ. Manage., 92: 2504–2512.

[11] Chen C., Li X., Zhao D., Tan X., Wang X. (2007) Adsorption kinetic, thermodynamic and desorption studies of Th(IV) on oxidized multi-wall carbon nanotubes. Colloid Surf. A: Physicochem. Eng. Asp., 302: 449–454.

[12] Haider S., Bukhari N., Park S. Y., Iqbal Y. (2011) Adsorption of bromo-phenol Blue from an aqueous solution onto thermally modified granular charcoal. Chem. Eng. Res. Des., 89: 23–28.

[13] Ricordel S., Taha S., Cisse I., Dorange G. (2001) Heavy metals removal by adsorption onto peanut husks carbon: Characterization, kinetic study and modeling. Sep. Purif. Technol., 24: 389–401.

[14] Tuzun I., Bayramoglu G., Yalcin E., Basaran G., Celik G., Arica M. Y. (2005) Equilibrium and kinetic studies on biosorption of Hg(II), Cd(II) and Pb(II) ions onto microalgae *Chlamydomonas Reinhardtii*. J. Environ. Manage., 77: 85–92.

[15] Sun Y. B., Yang S. T., Sheng G. D., Guo Z., Wang X. (2012) The removal of U(VI) from aqueous solution by oxidized multiwalled carbon nanotubes. J. Environ. Radioact., 105: 40–47.

[16] Kobya M., Demirbas E., Senturk E., Ince M. (2005) Adsorption of heavy metal ions from aqueous solutions by activated carbon prepared from apricot stone. Bioresour. Technol., 96: 1518–1521.

[17] Nadeem R., Nasir M. H., Hanif M. S. (2009) Pb(II) sorption by acidi-cally modified *Cicer arientinum* biomass. Chem. Eng. J., 150: 40–48.

[18] Duranoğlu D., Trochimczuk A. W., Beker U. (2012) Kinetics and thermodynamics of hexavalent chromium adsorption onto activated carbon derived from acrylonitrile–divinylbenzene copolymer. Chem. Eng. J., 187: 193–202.

[19] Bowman B. S. (2003) Applications of surfactant-modified zeolites to environmental remediation. Rev. Micropor. Mesopor. Mater., 61: 43–56.

[20] Xie J., Li C. J., Chi L. N., Wu D. Y. (2013) Chitosan modified zeolite as a versatile adsorbent for the removal of different pollutants from water. Fuel., 103: 480–485.

[21] Yu L., Gong J., Zeng C. F., Zhang L. X. (2013) Preparation of zeolite-A/chitosan hybrid composites and their bioactivities and antimicrobial activities. Mater. Sci. Eng. C., 33: 3652–3660.

[22] Wan Ngah W. S., Fatinathan S. (2010) Pb(II) biosorption using chitosan and chitosan derivatives beads: Equilibrium, ion exchange and mechanism studies. J. Environ. Sci., 22: 338–346.

[23] Soltani R. D., Khataee A. R., Safari M., Joo S. W. (2013) Preparation of bio-silica/chitosan nanocomposite for adsorption of a textile dye in aqueous solutions. Int. Biodeterior. Biodegradation., 85: 383–391.

[24] Aleksandra R. N., Sava J. V., Dušan G. A. (2013) Modification of chitosan by zeolite A and adsorption of Bezactive Orange 16 from aqueous solution. Composites: Part B., 53: 145–151.

[25] Gandhi M. R., Meenakshi S. (2012a) Preparation and characterization of La(III) encapsulated silica gel/chitosan composite and its metal uptake studies. J. Hazard. Mater., 203– 204: 29–37.

[26] Gandhi M. R., Meenakshi S. (2012b) Preparation and characterization of silica gel/chitosan composite for the removal of Cu(II) and Pb(II). Int. J. Biol. Macromol., 50: 650–657.

[27] Topallar H., Bayrak Y. (1998) The effect of temperature on the dynamic viscosity of acetone sunflower-seed oil mixtures. Turk. J. Chem., 22: 361–366.

[28] Sarin V., Pant K. K. (2006) Removal of chromium from industrial waste by using eucalyptus bark. Bioresour. Technol., 97: 15–20.

[29] Dahiya S., Tripathi R. M., Hegde A. G. (2008) Biosorption of lead and copper from aqueous solutions by pre-treated crab and arca shell biomass. Bioresour. Technol., 99: 179–187.

[30] Hall K. R., Eagleton L. C., Acrivos A., Vemeulen T. (1966) Pore and solid diffusion in fixed bed adsorption under constant pattern condition. Ind. Eng. Chem. Fund., 5: 213–223.

[31] Ho Y. S., McKay G. (1999) Pseudo-second order model for sorption processes. Process Biochem., 34: 451–465.

[32] Bhat S. V., Melo J. S., Chaugule B. B., D`Souza S. F. (2008) Biosorption characteristics of uranium from aqueous medium onto *Catenella repens*, a red alga. J. Hazard. Mater., 158: 628–635.

[33] Li Y. H., Xu C. L., Wei B. Q., Zhang X. F., Zheng M. X., Wu D. H., Ajayan P. M. (2002) Self-organized ribbons of aligned carbon nanotubes. Chem. Mater., 14: 483–485.

[34] Lu C. S., Chung Y. L., Chang K. F. (2005) Adsorption of trihalomethanes from water with carbon nanotube. Water Res., 39: 1183–1189.

[35] Shao D. D., Jiang Z. Q., Wang X. K. (2009) SDBS modified XC-72 carbon for the removal of Pb(II) from aqueous solutions. Plasma Process. Polym., 7: 552–560.

[36] Shao D. D., Jiang Z. Q., Wang X. K., Li J. X., Meng Y. D. (2009) Plasma induced grafting carboxymethyl cellulose on multiwalled carbon nanotubes for the removal of UO_2^{2+} from aqueous solution. J. Phys. Chem., B113: 860–864.

[37] Harmsen K. F., Haan A. M. (1980) Occurrence and behavior of uranium and thorium in soil and water. Neth. J. Agric. Sci., 28: 40–62.

[38] Hsi C-K. D., Langmuir D. (1985) Adsorption of uranyl onto ferric oxyhydroxides: Application of the surface complexation site-binding model. Geochim. Cosmochim. Acta., 49: 1931–1941.

[39] Katsoyiannis I. A. (2007) Carbonate effects and pH-dependence of uranium sorption onto bacteriogenic iron oxides: Kinetic and equilibrium studies. J. Hazard. Mater., B139: 31–37.

[40] Duquènea L., Tack F., Meers E., Baeten J., Wannijna J., Vandenhovem H. (2008) Effect of biodegradable amendments on uranium solubility in contaminated soils. Sci. Total Environ., 391: 26–33.

[41] Chingombe P., Saha B., Wakeman R. J. (2005) Surface modification and characterisation of a coal-based activated carbon. Carbon, 43: 3132–3143.

[42] Wang H., Zhou A., Peng F., Yu H., Chen L. (2007) Adsorption characteristic of acidified carbon nanotubes for heavy metal Pb(II) in aqueous solution. Mater. Sci. Eng., 466: 201–206.

[43] Ahmad A., Rafatullah M., Sulaiman O., Ibrahim M. H., Chii Y. Y., Siddique B. M. (2009) Removal of Cu (II) and Pb (II) ions from aqueous solutions by adsorption on sawdust of Meranti wood. Desalination, 247: 636–646.

[44] Ricordel S., Taha S., Cisse I., Dorange G. (2001) Heavy metals removal by adsorption onto peanut husks carbon: Characterization, kinetic study and modeling. Sep. Purif. Technol., 24: 389–401.

[45] Li Y. H., Wang S. G., Luan Z. K., Ding J., Xu C. L., Wu D. H. (2003) Adsorption of cadmium(II) from aqueous solution by surface oxidized carbon nanotubes. Carbon, 41: 1057–1062.

IntechOpen